Coulomb Resummation Near $t\bar{t}$ Threshold

Yingsheng Huang

Institute of High Energy Physics

Outlines

Fadin and Khoze [1987]

Melnikov et al. [1994]

Beneke et al. [2013]

The Idea

- For a process near the threshold of a specific fermion (i.e. $s \sim (2m_f)^2$), the exchange of Coulomb mode gluon is important, and for each order of the perturbative expansion, this part contributes an amount of approximately the same order.
- Perturbative expansion breaks down, resummation needed.
- To resum all Coulomb gluon exchange diagrams, one can use pNRQCD and convert the problem to a differential equation problem.

Fadin and Khoze [1987]

Fadin and Khoze [1987]

Coulomb resummation for top pair production in the threshold region can be traced back to '87[Fadin and Khoze, 1987].

$$
\begin{aligned}
\operatorname{Im} G_{E+i\Gamma_t}(0,0) = \frac{m_t^2}{4\pi}\Bigg[& \frac{k_+}{m_t} + \frac{2k_1}{m_t}\arctan\frac{k_+}{k_-} \\
& + \sum_{n=1}^{\infty} \frac{2\bar{k}_1^2}{m_t^2 n^4} \, \frac{\Gamma_t \bar{k}_1 n + k_+\left(n^2\sqrt{E^2+\Gamma_t^2} + \bar{k}_1^2/m_t\right)}{\left(E + \dfrac{\bar{k}_1^2}{m_t n^2}\right)^2 + \Gamma_t^2}\Bigg],
\end{aligned}
$$

$$
\bar{k}_1 = \frac{2}{3}\alpha_S m_t , \qquad k_\pm = \sqrt{\frac{m_t}{2}\left(\sqrt{E^2+\Gamma_t^2} \pm E\right)} . \quad (3)
$$

They discussed the total cross section of $e^+e^- \to t\bar{t}$ and the significance of this Coulomb effect at threshold varied with top mass (it was before the measurement of top mass in the '90s).

Coulomb resummation for top pair production in the threshold region can be traced back to '87[Fadin and Khoze, 1987].

$$\operatorname{Im} G_{E+i\Gamma_t}(0,0) = \frac{m_t^2}{4\pi}\left[\frac{k_+}{m_t} + \frac{2k_1}{m_t}\arctan\frac{k_+}{k_-}\right.$$
$$\left. + \sum_{n=1}^{\infty}\frac{2\bar{k}_1^2}{m_t^2 n^4}\,\frac{\Gamma_t\bar{k}_1 n + k_+\left(n^2\sqrt{E^2+\Gamma_t^2} + \bar{k}_1^2/m_t\right)}{\left(E + \frac{\bar{k}_1^2}{m_t n^2}\right)^2 + \Gamma_t^2}\right],$$
$$\bar{k}_1 = \frac{2}{3}\alpha_S m_t\,, \qquad k_{\pm} = \sqrt{\frac{m_t}{2}\left(\sqrt{E^2+\Gamma_t^2} \pm E\right)}\,. \quad (3)$$

They discussed the total cross section of $e^+e^- \to t\bar{t}$ and the significance of this Coulomb effect at threshold varied with top mass (it was before the measurement of top mass in the '90s).

The details of their calculation should be in *Sov.J.Nucl.Phys. 48 (1988) 309-313* which is nowhere to be found. *Strassler and Peskin [1991]* also gave a detailed description about $e^+e^- \to t\bar{t}$.

Melnikov et al. [1994]

They were mostly considering a pseudoscalar Higgs $A \to \gamma\gamma$ process in the context of MSSM, near $t\bar{t}$ threshold ($m_A = 2m_t + E$, $E \ll m_A$).

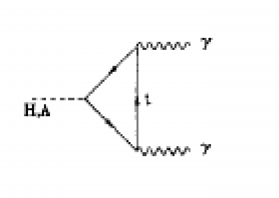

There're also W loops in $H \to \gamma\gamma$.

The diagrams are

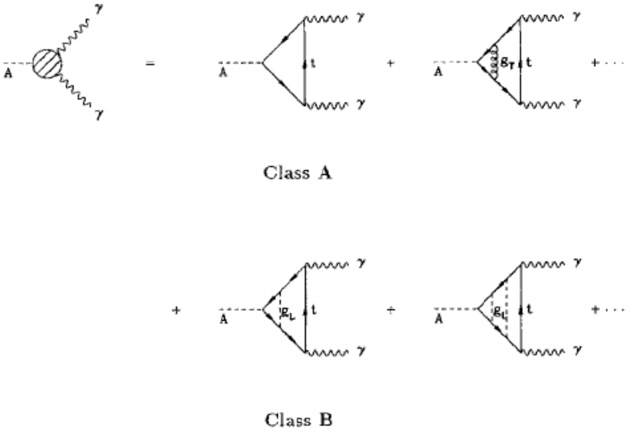

Fig. 5. Division of the gluon exchange diagrams contributing to the $A\gamma\gamma$ coupling into the classes A and B. g_T denotes transverse and g_L longitudinal gluon exchange in the Coulomb gauge

The $A \to \gamma\gamma$ amplitude is expressed as

$$F_t^A = b \int \frac{d^4 p_t}{(2\pi)^4} \operatorname{Tr} \{ S_t(p_t) \Gamma_{At\bar{t}} S_t(p_{\bar{t}}) \Gamma_{t\bar{t}\gamma\gamma} \} , \qquad (24)$$

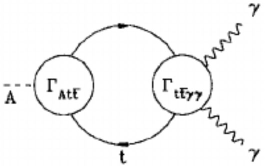

Fig. 6. Diagrammatic representation of the $A\gamma\gamma$ coupling in terms of the vertex operators $\Gamma_{t\bar{t}\gamma\gamma}$ and $\Gamma_{At\bar{t}}$

The top propagator with width is

$$S_t(p) = \frac{1+\gamma_0}{2} \frac{\mathrm{i}}{\varepsilon - \dfrac{\mathbf{p}^2}{m_t} + \mathrm{i}\dfrac{\Gamma_t}{2}}, \quad \text{with} \quad p = (m_t + \varepsilon, \mathbf{p}) . \quad (25)$$

The $A \to \gamma\gamma$ amplitude is expressed as

$$F_t^A = b \int \frac{d^4 p_t}{(2\pi)^4} \mathrm{Tr} \left\{ S_t(p_t) \Gamma_{At\bar{t}} S_t(p_{\bar{t}}) \Gamma_{t\bar{t}\gamma\gamma} \right\}, \qquad (24)$$

Take the leading order of $\Gamma_{At\bar{t}}$ which is just a coupling, and take $\Gamma_{t\bar{t}\gamma\gamma}$ to include all Coulomb gluon exchanges.

$$\Gamma_{t\bar{t}\gamma\gamma}(\mathbf{p}, E) = \Gamma^0_{t\bar{t}\gamma\gamma} \left\{ \frac{\mathbf{p}^2}{m_t} - E - i\Gamma_t \right\} G_t(\mathbf{p}; E), \qquad (26)$$

$\Gamma^0_{t\bar{t}\gamma\gamma}$ is also the coupling of $t\bar{t} \to \gamma\gamma$.

Solve the Schrödinger equation

$$
\begin{aligned}
(\hat{H} - E - \mathrm{i}\Gamma_t)\, G_t(\mathbf{r}, \mathbf{r}'; E) &= \delta(\mathbf{r} - \mathbf{r}'), \\
\text{with } \hat{H} &= -\frac{\nabla^2}{m_t} + V(r), \\
V(r) &= -\frac{4}{3}\frac{\alpha_s}{r}, \\
G_t(\mathbf{p}; E) &= \int \mathrm{d}^3\mathbf{r}\, G_t(\mathbf{r}, \mathbf{r}' = 0; E)\, e^{-\mathrm{i}\mathbf{p}\mathbf{r}}.
\end{aligned}
\tag{27}
$$

After substituting (25) and (26) into (24) the p_t^0–integration can be performed explicitly by taking the residue of the pole at $p_t^0 = m_t + \mathbf{p}^2/m_t - \mathrm{i}\Gamma_t/2$. Adding the contributions of class B and those of the class A diagrams we obtain as the final result

$$F_t^A(E) = A + B\ G_t(0, 0; E), \tag{28}$$

where A and B are real constants, which can be expanded in a perturbative series:

$$A = \sum_{n=0}^{\infty} A_n \left(\frac{\alpha_s}{\pi}\right)^n, \quad B = \sum_{n=0}^{\infty} B_n \left(\frac{\alpha_s}{\pi}\right)^n. \tag{29}$$

The coefficients A_n and B_n can be determined from the comparison with the usual perturbative QCD corrections. The calculation of the amplitude F_W^H is performed in an analogous way without the contribution of the Coulomb potential $V(r)$ by taking into account the W decay width Γ_W only.

To do this matching they have some predetermined results

and t–quark) as shown in Fig.1. The top quark and W amplitudes read in lowest order [4–6]

$$
\begin{aligned}
F_t^H &= -2\tau[1 + (1-\tau) f(\tau)] , \\
F_W^H &= 3\tau + 2 - 3\tau(\tau - 2) f(\tau) , \\
F_t^A &= \tau f(\tau) .
\end{aligned}
\tag{1}
$$

The scaling variable is defined as $\tau = 4m_i^2/m_\phi^2$, where m_i denotes the loop–particle mass and m_ϕ the corresponding Higgs mass, and

$$
f(\tau) = \begin{cases} \arcsin^2 \dfrac{1}{\sqrt{\tau}}, & \tau \geqq 1, \\ -\dfrac{1}{4}\left(\log \dfrac{1+\sqrt{1-\tau}}{1-\sqrt{1-\tau}} - i\pi\right)^2, & \tau < 1. \end{cases}
\tag{2}
$$

And by expanding F_t^A near $\tau = 1$, the value of A_n and B_n is obtained.

Result of G

The result of a stable top is

$$G_t(0,0;E) = -\frac{m_t p}{4\pi} + \frac{m_t p_0}{2\pi}\log\left(\frac{m_t}{p}D\right) + \frac{m_t p_0^2}{2\pi}\sum_{n=1}^{\infty}\frac{1}{n(np-p_0)}, \tag{8}$$

with $p_0 = 2/3 m_t \alpha_s$ and $p = \sqrt{m_t(-E-\mathrm{i}\varepsilon)}$.

D is a real renormalization artifact.

To get a result with finite width, one perform the substitution

$$E \to E + \mathrm{i}\Gamma\,, \tag{11}$$

and

$$p \to p = \sqrt{m(-E-\mathrm{i}\Gamma)} = p_- - \mathrm{i}p_+$$

$$p_\pm = \sqrt{m/2(\sqrt{E^2+\Gamma^2} \pm E)}.$$

Result of G

The result with finite top width is

$$\Re e\; G_t(0,0;E+\mathrm{i}\Gamma_t) = -\frac{m_t p_-}{4\pi} + \frac{m_t p_0}{4\pi}\log\left(\frac{m_t^2}{p_+^2+p_-^2}D^2\right) + \frac{m_t p_0^2}{2\pi}\sum_{n=1}^{\infty}\frac{p_- - p_n}{n^2((p_- - p_n)^2 + p_+^2)},$$

$$\Im m\; G_t(0,0;E+\mathrm{i}\Gamma_t) = \frac{m_t p_+}{4\pi} + \frac{m_t p_0}{2\pi}\arctan\frac{p_+}{p_-} + \frac{m_t p_0^2}{2\pi}\sum_{n=1}^{\infty}\frac{p_+}{n^2((p_- - p_n)^2 + p_+^2)}, \quad (12)$$

with $p_n = \frac{p_0}{n}$, and $p_0 = \frac{2}{3} m_t \alpha_s$.

and

$$p_\pm = \sqrt{m/2(\sqrt{E^2+\Gamma^2} \pm E)}.$$

Result of G

The summation in (8) is evaluated to be

$$\sum_{i=1}^{n} \frac{1}{n(np - p_0)} = -\frac{\psi^{(0)}\left(1 - \frac{p_0}{p}\right) + \gamma_E}{p_0} = -\frac{H_{-p_0/p}}{p_0} \tag{1}$$

where $H_n \equiv \left(\sum_{i=1}^{n} 1/i\right)$ is the harmonic number.

In [Bharucha et al., 2016] the summation isn't actually done to all order:

> orders[2] [8]. The three terms in the above expressions correspond to the lowest order contribution, a single Coulombic photon exchange and a sum over contributions involving the exchange of $n+1$ Coulombic photons. The position of the first pole in E_f can be obtained by inspecting the denominator of the $n=1$ contribution to the last terms of the equations above. Although the sum in n runs from 1 to ∞, the sum converges rather quickly and, in reality, it is sufficient for our purposes to calculate up to $n = 100$.

Compare amplitudes

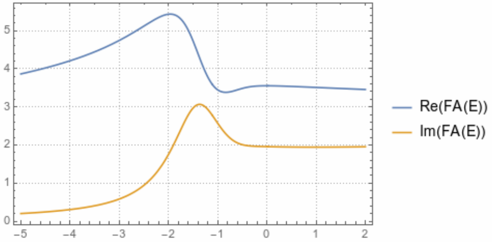

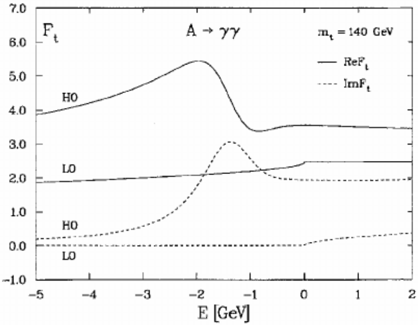

Shape of the Green function

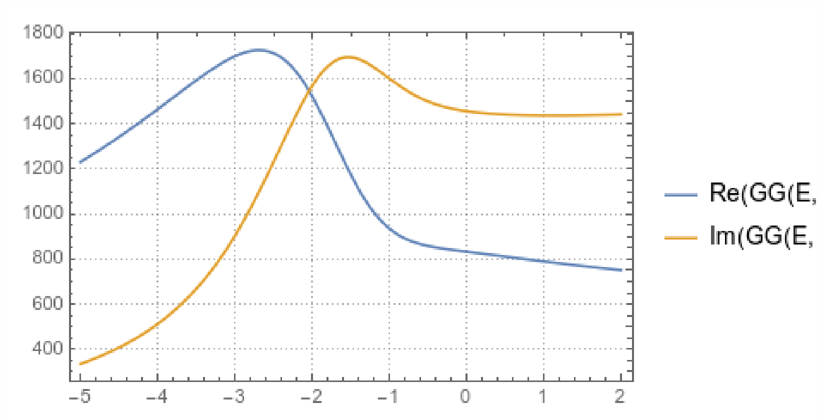

Determine A, B

To determine the leading A and B: Take $A \to \gamma\gamma$ as an example,

$$G_t(E) = -\frac{m_t\sqrt{m_t(-E - i\epsilon)}}{4\pi} \tag{2}$$

And $F_t^A = \tau f(\tau)$ is expanded to be

$$\frac{\pi^2}{4} - i\pi\sqrt{\tau - 1} + \mathcal{O}(\tau - 1) \tag{3}$$

The latter one, according to the definition of τ is expressed as

$$-\pi\sqrt{\frac{-E - i\epsilon}{m_t}} \tag{4}$$

which leads to the final result

$$A_t^A = \frac{\pi^2}{4}, \quad B_t^A = \frac{4\pi^2}{m_t^2}.$$

Further QCD Corrections

1. QCD radiative corrections to the static heavy quark–antiquark potential $V(r)$ [23, 24],
2. QCD radiative corrections to the Born width of the top quark [25],
3. hard QCD radiative corrections to the $H \to t\bar{t}$ and $t\bar{t} \to \gamma\gamma$ amplitudes [26, 27].

The 1st one is done by considering the running of α_S.

The 2nd one is not considered (too small).

The 3rd one: see next page

The QCD radiative corrections to the Born width of the top quark were calculated in [25] and are negligible in our analysis. The third contribution leads to a correction to the constant B in (4)

$$B = B_0\left(1 + b\frac{\alpha_s}{\pi}\right). \tag{20}$$

The coefficient b can be obtained analytically from the well–known results of [26] and [27], because the real corrections to their results belong to a P–wave contribution and therefore vanish at threshold. The hard corrections at threshold to the process $t\bar{t} \to \gamma\gamma$ are given by [26]

$$1 - \frac{\alpha_s(2m_t)}{\pi}\left[\frac{C_F}{2}\left(5 - \frac{\pi^2}{4}\right)\right], \tag{21}$$

and the corresponding ones to $A \to t\bar{t}$ by [27]

$$1 - \frac{\alpha_s(2m_t)}{\pi}\left(3\,\frac{C_F}{2}\right). \tag{22}$$

The coefficient b is determined by the sum of both contributions:

$$b = -\frac{C_F}{2}\left(8 - \frac{\pi^2}{4}\right), \tag{23}$$

Beneke et al. [2013]

Diagrams

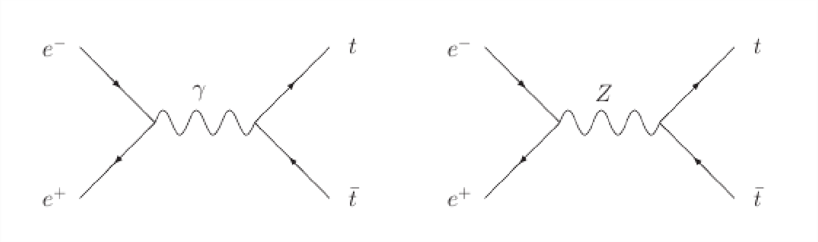

Heavy quark current correlation function

$$
\begin{aligned}
\Pi_{\mu\nu}^{(X)}(q^2) &= i \int d^4x\, e^{iq\cdot x}\, \langle 0|T(j_\mu^{(X)}(x) j_\nu^{(X)}(0))|0\rangle \\
&= (q_\mu q_\nu - q^2 g_{\mu\nu})\, \Pi^{(X)}(q^2) + q_\mu q_\nu \Pi_L^{(X)}(q^2), \qquad (2.1)
\end{aligned}
$$

for the vector current $j_\mu^{(v)} = \bar{t}\gamma_\mu t$ and the axial vector current $j_\mu^{(a)} = \bar{t}\gamma_\mu\gamma_5 t$. The cross section is then given by

$$
\begin{aligned}
\sigma_{t\bar{t}X} = \sigma_0 \times 12\pi\, \mathrm{Im}\Bigg[& e_t^2 \Pi^{(v)}(q^2) - \frac{2q^2}{q^2 - M_Z^2} v_e v_t e_t \Pi^{(v)}(q^2) \\
& + \left(\frac{q^2}{q^2 - M_Z^2} \right)^2 (v_e^2 + a_e^2)(v_t^2 \Pi^{(v)}(q^2) + a_t^2 \Pi^{(a)}(q^2)) \Bigg], \qquad (2.2)
\end{aligned}
$$

where $\sigma_0 = 4\pi\alpha_{\mathrm{em}}^2/(3s)$ is the high-energy limit of the $\mu^+\mu^-$ production cross section, $s = q^2$ the center-of-mass energy squared, and M_Z the Z-boson mass. $e_t = 2/3$ denotes the top quark electric charge in units of positron charge and α_{em} is the electromagnetic coupling. The vector and axial-vector couplings of fermion f to the Z-boson are given by

$$
v_f = \frac{T_3^f - 2e_f \sin^2\theta_w}{2\sin\theta_w \cos\theta_w}, \qquad a_f = \frac{T_3^f}{2\sin\theta_w \cos\theta_w}, \qquad (2.3)
$$

Before going into the details of the Lagrangian and power counting we briefly sketch the result. As will be shown below the expansion of the vector current $j^{(v)\,\mu}$ in terms of the non-relativistic fields is given by

$$j^{(v)\,i} = c_v\,\psi^\dagger\sigma^i\chi + \frac{d_v}{6m^2}\,\psi^\dagger\sigma^i\,\mathbf{D}^2\chi + \ldots, \tag{3.1}$$

where the hard matching coefficients c_v, d_v have perturbative expansions in α_s. In the "rest frame" $q^\mu = (2m+E,\mathbf{0})$, eq. (2.1) implies $\Pi^{(v)}_{ij} = q^2\delta_{ij}\,\Pi^{(v)}(q^2)$, so

$$\Pi^{(v)}(q^2) = \frac{1}{(d-1)q^2}\,\Pi^{(v)}_{ii} = \frac{N_c}{2m^2}\,c_v\left[c_v - \frac{E}{m}\left(c_v + \frac{d_v}{3}\right)\right]G(E) + \ldots, \tag{3.2}$$

where the neglected terms on the right-hand side include a subtraction term that does not contribute to the imaginary part of $\Pi^{(v)}(q^2)$ as well as terms beyond the third order (NNNLO). The important quantity is the two-point function of the non-relativistic current

$$G(E) = \frac{i}{2N_c(d-1)}\int d^dx\,e^{iEx^0}\,\langle 0|\,T(\,[\chi^\dagger\sigma^i\psi](x)\,[\psi^\dagger\sigma^i\chi](0))|0\rangle_{|\text{NRQCD}}\,, \tag{3.3}$$

where now the matrix element must be evaluated in non-relativistic QCD (NRQCD). The terms proportional to E in (3.2) arise from expanding the prefactor $1/q^2$ and from

Match to NRQCD

Similar relations hold for the axial-vector contribution to the cross section (2.2), which arises from Z-boson exchange. The axial-vector current $j^{(a)\,\mu} = \bar{t}\gamma^\mu\gamma_5 t$ is represented in NRQCD by the expansion

$$j^{(a)\,i} = \frac{c_a}{2m}\,\psi^\dagger\left[\sigma^i, (-i)\boldsymbol{\sigma}\cdot\mathbf{D}\right]\chi + \ldots, \tag{3.4}$$

with hard matching coefficient c_a. As is the case for the vector current, only the spatial components of the current contribute to the cross section, since the lepton tensor from the e^+e^- initial state is transverse to both initial state momenta when the electron mass is neglected. Only the leading term in the $1/m$ expansion is needed for NNNLO accuracy, since the derivative in the leading current implies the well-known P-wave velocity suppression. The QCD correlation function is then given by the expression

$$\Pi^{(a)}(q^2) = \frac{1}{(d-1)q^2}\,\Pi^{(a)}_{ii} \tag{3.5}$$

$$= \frac{N_c}{8m^4}\,c_a^2 \times \frac{i}{2N_c(d-1)}\int d^dx\, e^{iEx^0}\,\langle 0|\,T(\,[\psi^\dagger\Gamma^i\chi]^\dagger(x)\,[\psi^\dagger\Gamma^i\chi](0))|0\rangle_{|\mathrm{NRQCD}} + \ldots,$$

where $\Gamma^i = (-i)[\sigma^i, \boldsymbol{\sigma}\cdot\mathbf{D}]$.

As will be discussed below no further matching of the non-relativistic vector current is needed, that is $\psi^\dagger \sigma^i \chi_{|\mathrm{NRQCD}} = \psi^\dagger \sigma^i \chi_{|\mathrm{PNRQCD}}$ to the required accuracy. Thus, instead of (3.3), we have to calculate

$$G(E) = \frac{i}{2N_c(d-1)} \int d^d x\, e^{iEx^0} \langle 0|\, T(\, [\chi^\dagger \sigma^i \psi](x)\, [\psi^\dagger \sigma^i \chi](0))|0\rangle_{|\mathrm{PNRQCD}}\,, \tag{4.3}$$

where now the matrix element must be evaluated to third-order in PNRQCD perturbation theory.

Lagrangian:

$$\begin{aligned}
\mathcal{L}_{\mathrm{PNRQCD}} = {} & \psi^\dagger \Big(i\partial_0 + g_s A_0(t,\mathbf{0}) + \frac{\boldsymbol{\partial}^2}{2m} + \frac{\boldsymbol{\partial}^4}{8m^3} \Big) \psi + \chi^\dagger \Big(i\partial_0 + g_s A_0(t,\mathbf{0}) - \frac{\boldsymbol{\partial}^2}{2m} - \frac{\boldsymbol{\partial}^4}{8m^3} \Big) \chi \\
& + \int d^{d-1}\mathbf{r} \, \Big[\psi_a^\dagger \psi_b \Big](x+\mathbf{r})\, V_{ab;cd}(r, \boldsymbol{\partial}) \, \Big[\chi_c^\dagger \chi_d \Big](x) \\
& - g_s \psi^\dagger(x) \mathbf{x} \cdot \mathbf{E}(t,\mathbf{0}) \psi(x) - g_s \chi^\dagger(x) \mathbf{x} \cdot \mathbf{E}(t,\mathbf{0}) \chi(x),
\end{aligned} \tag{4.1}$$

where

$$V_{ab;cd}(r, \boldsymbol{\partial}) = T^A_{ab} T^A_{cd} V_0(r) + \delta V_{ab;cd}(r, \boldsymbol{\partial}) \tag{4.2}$$

with $V_0 = -\alpha_s/r$ the tree-level colour Coulomb potential. The PNRQCD Lagrangian consists of kinetic terms (first line; including the relativistic corrections proportional to $\boldsymbol{\partial}^4/m^3$), heavy-quark potential interactions (second line) and an ultrasoft interaction that contributes first at third order. The heavy-quark potentials generated in the

The Lippmann-Schwinger equation for the leading order Green function G_0 is

$$\left(\frac{\mathbf{p}^2}{m} - E\right) G_0^{(R)}(\mathbf{p}, \mathbf{p}'; E) + \tilde{\mu}^{2\epsilon} \int \frac{d^{d-1}\mathbf{k}}{(2\pi)^{d-1}} \frac{4\pi D_R \alpha_s}{\mathbf{k}^2} G_0^{(R)}(\mathbf{p} - \mathbf{k}, \mathbf{p}'; E)$$
$$= (2\pi)^{d-1} \delta^{(d-1)}(\mathbf{p} - \mathbf{p}')\,, \tag{4.5}$$

where R denotes color state, $D_1 = -C_F$ and $D_8 = -\left(C_F - C_A/2\right)$.

$$G_0^{(R)}(\mathbf{r}, \mathbf{r}'; E) = \int \frac{d^{d-1}\mathbf{p}}{(2\pi)^{d-1}} \frac{d^{d-1}\mathbf{p}'}{(2\pi)^{d-1}} e^{i\mathbf{p}\cdot\mathbf{r}}\, e^{-i\mathbf{p}'\cdot\mathbf{r}'}\, G_0^{(R)}(\mathbf{p}, \mathbf{p}'; E) \tag{4.6}$$

In 4-d the corresponding Schrödinger equation is

$$\left(-\frac{\nabla_{(r)}^2}{m} + \frac{D_R \alpha_s}{r} - E\right) G_0^{(R)}(\mathbf{r}, \mathbf{r}'; E) = \delta^{(3)}(\mathbf{r} - \mathbf{r}')\,. \tag{4.7}$$

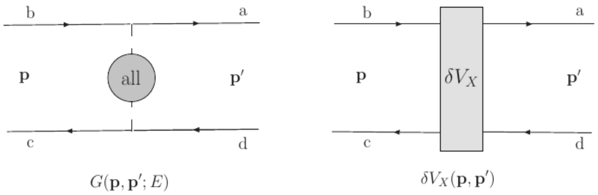

Figure 7: PNRQCD Feynman rules.

The vertex associated with the insertion of a perturbation potential $\delta V_{ab;cd}(\mathbf{p}, \mathbf{p}')$ in momentum space is given by

$$i\delta V_{ab;cd}(\mathbf{p}, \mathbf{p}')\,, \tag{4.8}$$

and internal relative momenta $\mathbf{p}_i$ are integrated over with measure $\tilde{\mu}^{2\epsilon} \int d^{d-1}\mathbf{p}_i/(2\pi)^{d-1}$.

$$\int \left[\prod_i \frac{d^{d-1}\mathbf{p}_i}{(2\pi)^{d-1}} \right] iG_0(\mathbf{p}_1, \mathbf{p}_2; E) i\delta V_1(\mathbf{p}_2, \mathbf{p}_3) iG_0(\mathbf{p}_3, \mathbf{p}_4; E)\, i\delta V_2(\mathbf{p}_4, \mathbf{p}_5) iG_0(\mathbf{p}_5, \mathbf{p}_6; E)\ \ldots \tag{4.10}$$

Green function: Higher Order

For higher orders, some methods are discussed in [Hoang et al., 2000]:

- ☐ Hoang–Teubner (HT), solved the NNLO Schr¨odinger equation exactly in momentum space representation.
- ☐ Melnikov–Yelkhovsky–Yakovlev–Nagano–Ota–Sumino (MYYNOS), solved the NNLO Schr¨odinger equation exactly in coordinate space representation.

  expanded in r_0. Only logarithms of r_0 were kept and inverse powers of r_0 were discarded. The value of r_0 was chosen of the order of the inverse top quark mass. The short-distance coefficient

- ☐ Penin–Pivovarov (PP), solved the NNLO Schr¨odinger equation perturbatively in coordinate space representation.
- ☐ Beneke–Signer–Smirnov (BSS), solved the NNLO Schr¨odinger equation perturbatively using dim-reg.

Consider the sum of all ladder diagrams:

$$H(\mathbf{p},\mathbf{p}';E) = \sum_{n=0}^{\infty} C_F^{n+1} \int \left[\prod_{i=1}^{n} \frac{d^d k_i}{(2\pi)^d}\right] \frac{(ig_s)^2 i}{(\mathbf{k}_1-\mathbf{k}_0)^2} \frac{(ig_s)^2 i}{(\mathbf{k}_2-\mathbf{k}_1)^2} \cdots \frac{(ig_s)^2 i}{(\mathbf{k}_{n+1}-\mathbf{k}_n)^2}$$
$$\cdot \prod_{i=1}^{n} \frac{i}{\frac{E}{2}+k_i^0-\frac{(\mathbf{p}+\mathbf{k}_i)^2}{2m}+i\epsilon} \frac{-i}{\frac{E}{2}-k_i^0-\frac{(\mathbf{p}+\mathbf{k}_i)^2}{2m}+i\epsilon}, \tag{4.11}$$

where we define $\mathbf{k}_{n+1} = \mathbf{p}'-\mathbf{p}$ and $\mathbf{k}_0 \equiv 0$. We perform the integrations over the loop

After integrated out k^0s

$$H(\mathbf{p},\mathbf{p}';E) = i\sum_{n=0}^{\infty} (-g_s^2 C_F)^{n+1} \int \left[\prod_{i=1}^{n} \frac{d^{d-1}\mathbf{k}_i}{(2\pi)^{d-1}}\right] \frac{1}{\mathbf{k}_1^2}$$
$$\times \prod_{i=1}^{n} \frac{1}{(\mathbf{k}_{i+1}-\mathbf{k}_i)^2(E-\frac{(\mathbf{p}+\mathbf{k}_i)^2}{2m}+i\epsilon)}. \tag{4.12}$$

Next we multiply the propagator factors $(-i)/(E+i\epsilon-\mathbf{p}^2/m)$ for the external pairs of lines and add the zero-Coulomb exchange graph. Multiplying by $(-i)$ this defines

$$G_0(\mathbf{p},\mathbf{p}';E) = -\frac{(2\pi)^{d-1}\delta^{(d-1)}(\mathbf{p}'-\mathbf{p})}{E+i\epsilon-\frac{\mathbf{p}^2}{m}} + \frac{1}{E+i\epsilon-\frac{\mathbf{p}^2}{m}}\, iH(\mathbf{p},\mathbf{p}';E)\, \frac{1}{E+i\epsilon-\frac{\mathbf{p}'^2}{m}}\,. \quad (4.13)$$

which satisfies the Lippmann-Schwinger equation for G_0. Higher orders

$$G(E) = \int \frac{d^{d-1}\mathbf{p}}{(2\pi)^{d-1}}\frac{d^{d-1}\mathbf{p}'}{(2\pi)^{d-1}}\Bigg[G_0^{(1)}(\mathbf{p},\mathbf{p}';E)$$

$$+ \int \frac{d^{d-1}\mathbf{p}_1}{(2\pi)^{d-1}}\frac{d^{d-1}\mathbf{p}_1'}{(2\pi)^{d-1}}\, G_0^{(1)}(\mathbf{p},\mathbf{p}_1;E)\, i\delta V(\mathbf{p}_1,\mathbf{p}_1')\, iG_0^{(1)}(\mathbf{p}_1',\mathbf{p}';E) + \ldots \Bigg]\,, \quad (4.14)$$

The spin indices is included

$$\delta V = \frac{1}{2(d-1)}\,\sigma^i_{\alpha\alpha'}\,\delta V_{\alpha\beta';\alpha'\beta}\,\sigma^i_{\beta\beta'}\,, \quad (4.15)$$

with normalization

An integral representation for the position space Coulomb Green function is

$$G_0(\mathbf{r},\mathbf{r}';E) = -\frac{m}{4\pi\Gamma(1+\lambda)\Gamma(1-\lambda)}\int_0^1 dt\int_1^\infty ds\,[s(1-t)]^\lambda[t(s-1)]^{-\lambda}$$
$$\times\frac{\partial^2}{\partial t\partial s}\left(\frac{ts}{|s\mathbf{r}-t\mathbf{r}'|}\,e^{-\sqrt{-mE}\,((1-t)r'+(s-1)r+|s\mathbf{r}-t\mathbf{r}'|)}\right), \qquad (4.46)$$

valid for $r > r'$, where $r = |\mathbf{r}|$, $r' = |\mathbf{r}'|$ [99]. For $r < r'$ exchange $\mathbf{r} \leftrightarrow \mathbf{r}'$ in the above expression. Putting one of the arguments to zero, this simplifies to

$$G_0(0,r;E) = \frac{m\sqrt{-mE}}{2\pi}\,e^{-\sqrt{-mE}\,r}\int_0^\infty ds\,e^{-2rs\sqrt{-mE}}\left(\frac{1+s}{s}\right)^\lambda, \qquad (4.47)$$

which depends only on $r = |\mathbf{r}|$. We use this form of the Coulomb Green function mainly for propagators connecting to the external current vertex, in which case (4.47) applies.

Explicit forms of the propagator (Coulomb Green function)

For the general case of a propagator in between two potential insertions the representation of the position-space Green function in terms of Laguerre polynomials $L_n^{(2l+1)}(x)$ [100,101] turns out to be most useful. In this representation one first performs a partial wave expansion

$$G_0(\mathbf{r},\mathbf{r}';E) = \sum_{l=0}^{\infty} (2l+1)\, P_l\left(\frac{\mathbf{r}\cdot\mathbf{r}'}{rr'}\right) G_{[l]}(r,r';E)\,, \tag{4.48}$$

where $P_l(z)$ are the Legendre polynomials. The partial-wave Green functions read

$$G_{[l]}(r,r';E) = \frac{mp}{2\pi}\,(2pr)^l(2pr')^l\, e^{-p(r+r')} \sum_{s=0}^{\infty} \frac{s!\, L_s^{(2l+1)}(2pr) L_s^{(2l+1)}(2pr')}{(s+2l+1)!(s+l+1-\lambda)}\,, \tag{4.49}$$

where $p=\sqrt{-mE}$, and the Laguerre polynomials are defined by

$$L_s^{(\alpha)}(z) = \frac{e^z z^{-\alpha}}{s!}\left(\frac{d}{dz}\right)^s \left[e^{-z} z^{s+\alpha}\right]. \tag{4.50}$$

END

Questions?

Backup

References

Beneke, M., Kiyo, Y., and Schuller, K. (2013). Third-order correction to top-quark pair production near threshold I. Effective theory set-up and matching coefficients.

Bharucha, A., Djouadi, A., and Goudelis, A. (2016). Threshold enhancement of diphoton resonances. *Phys. Lett.*, B761:8–15.

Fadin, V. S. and Khoze, V. A. (1987). Threshold behavior of the cross section for the production of t quarks in e+e- annihilation. *JETP Letters*, 46(11):525.

Hoang, A. H. et al. (2000). Top - anti-top pair production close to threshold: Synopsis of recent NNLO results. *Eur. Phys. J.direct*, 2(1):3.

Melnikov, K., Spira, M., and Yakovlev, O. I. (1994). Threshold effects in two photon decays of Higgs particles. *Z. Phys.*, C64:401–406.

Strassler, M. J. and Peskin, M. E. (1991). The Heavy top quark threshold: QCD and the Higgs. *Phys. Rev.*, D43:1500–1514.